

**Zeitschrift:** IABSE publications = Mémoires AIPC = IVBH Abhandlungen

**Band:** 29 (1969)

**Artikel:** Precision of finite element method in plane stress

**Autor:** Hrennikoff, A.

**DOI:** <https://doi.org/10.5169/seals-22922>

#### **Nutzungsbedingungen**

Die ETH-Bibliothek ist die Anbieterin der digitalisierten Zeitschriften auf E-Periodica. Sie besitzt keine Urheberrechte an den Zeitschriften und ist nicht verantwortlich für deren Inhalte. Die Rechte liegen in der Regel bei den Herausgebern beziehungsweise den externen Rechteinhabern. Das Veröffentlichen von Bildern in Print- und Online-Publikationen sowie auf Social Media-Kanälen oder Webseiten ist nur mit vorheriger Genehmigung der Rechteinhaber erlaubt. [Mehr erfahren](#)

#### **Conditions d'utilisation**

L'ETH Library est le fournisseur des revues numérisées. Elle ne détient aucun droit d'auteur sur les revues et n'est pas responsable de leur contenu. En règle générale, les droits sont détenus par les éditeurs ou les détenteurs de droits externes. La reproduction d'images dans des publications imprimées ou en ligne ainsi que sur des canaux de médias sociaux ou des sites web n'est autorisée qu'avec l'accord préalable des détenteurs des droits. [En savoir plus](#)

#### **Terms of use**

The ETH Library is the provider of the digitised journals. It does not own any copyrights to the journals and is not responsible for their content. The rights usually lie with the publishers or the external rights holders. Publishing images in print and online publications, as well as on social media channels or websites, is only permitted with the prior consent of the rights holders. [Find out more](#)

**Download PDF:** 09.02.2026

**ETH-Bibliothek Zürich, E-Periodica, <https://www.e-periodica.ch>**

## Precision of Finite Element Method in Plane Stress

*Précision de la méthode des éléments finis dans le plan des tensions*

*Genauigkeit der endlichen Elemente für ebene Spannungszustände*

A. HRENNIKOFF

Sc. D., Research Professor of Civil Engineering. The University of British Columbia,  
Vancouver, B.C., Canada

### General

The method of Finite Element is a recognized tool of structural analysis of two and three dimensional elastic continua. In this method the loaded structure is replaced by a model consisting of numerous finite elements or cells endowed with suitable elastic properties. The model is analyzed by computer, whose solution on reduction of the cell size, converges to the true solution of the structure.

Although many types of cells composing the model may lead to correct results, some are inferior to others with regard to the progress of convergence, thus requiring a finer mesh and a longer computer time for the same degree of accuracy. The present investigation, restricted to the problems of plane stress, sets forth the desirable features of cells and names their superior types. Several procedures for determination of stresses are examined closely. The conclusions are illustrated on the examples.

### Necessary Requirements of Cells in Plane Stress

The cells composing the model are polygonal in shape, usually triangular or quadrilateral; they are joined to each other at the corners or nodes. The external loads must be applied to the model only at the nodes. Solution of the model involves determination of the nodal displacements, and this requires generation of the stiffness matrix of the cell  $\{K\}$ , relating the nodal load vector  $\{P\}$  with the nodal displacement vector  $\{\delta\}$  by the equation:

$$\{P\} = \{K\}\{\delta\}.$$

With two degrees of freedom per node the matrix  $\{K\}$  has  $6 \times 6$  size in triangular cells and  $8 \times 8$  in quadrilateral.

It must be clearly understood that a finite element is not a piece of plate held in deformed shape by the corner forces. Model made of such pieces of plate would be much too deformable. Actually, the finite element is something of a mathematical abstraction. This is how its nature may be explained. An expanse of plate, with the shape of the required finite element sketched on it, may be brought into a deformed state, in which one corner of the sketched figure is displaced a unit distance in  $x$  or  $y$  direction, while the other corners remain in the original locations. Such deformation may be accomplished by superposition in an unlimited plate of several simple stress conditions combined with additional free body movements. The sketched shape may be cut out of the plate and preserved in its deformed condition by application of appropriate edge stresses along its outline. The transformation of this piece of plate into the finite element is brought about by replacement of its edge stresses with statically equivalent  $X$  and  $Y$  force components applied at its several nodes. These components become the terms of the stiffness matrix of the cell in the column corresponding to the assumed unit nodal displacement.

Two different methods of converting the edge stresses into the equivalent corner forces are available: that of ordinary statics in which the edge stresses are transferred to the adjacent nodes only, and another one based on the energy considerations. In unsymmetrical quadrilaterals the two methods result in different stiffness matrices.

Remembering that the number of degrees of freedom of the corners is six in the triangles and eight in the quadrilaterals, and that the possible number of the free body movements is three, one can see that  $6 - 3 = 3$  different stress conditions are required in the triangles and  $8 - 3 = 5$  in the quadrilaterals, in order to effect the single corner movements in the process of generation of the stiffness matrix. The necessary requirement is that these 3 or 5 stress conditions must include the following three: uniform strain (or stress) in  $x$  direction, same in  $y$  direction, and uniform shear strain in  $x$  and  $y$  directions. Without satisfying these three conditions the stiffness matrices may not be valid. A quadrilateral cell evidently must satisfy two additional stress conditions. In rectangles these conditions have been taken as uniform flexures with stresses in  $x$  and  $y$  directions [1], and some others [2].

The computer generates the stiffness matrix of the whole model and solves the numerous simultaneous equations for the nodal displacements.

In the triangular cells and the rectangular ones of Ref. [2], continuity of the adjacent cells is preserved not only at the nodes, but also all along the boundaries. In rectangular cells of Ref. [1] on the other hand the adjacent edges of the neighbouring cells do not stay together. The significance of the edge continuity is a subject of disagreement, with some investigators insisting on its vital importance for the validity of the method. It appears that this

view has arisen from misinterpretation of the demonstration of the finite element method by the Rayleigh-Ritz energy principle. Actually however, recourse to this principle is not needed. A finite element model made of mesh of infinitesimal size, with cells obeying the three conditions of uniform strain, becomes in effect an assembly of interacting molecules, satisfying the same differential equations of elasticity as the plate prototype, and resulting in the same true solution, irrespective of whether or not the adjacent edges of the cells coincide. A solution involving finite size cells naturally is not exact, but the error disappears in the limit as the cells reduce to zero size.

### **Determination of Stresses**

Determination of nodal displacements is only the first phase in the analysis of the plate; stresses are also required, and normally engineers are more interested in stresses than in displacements. The subject of stress determination has not received the attention which it deserves, and it will be discussed here in detail.

Stresses may be found either by using the nodal displacements or the nodal force concentrations, two procedures being available for each of these two methods.

#### **Method 1a of Nodal Displacements**

This is the method taken for granted by the great majority of investigators. It makes use of the above described correspondence between the finite element and the deformed piece of plate, from which the former was evolved. With the displacements of all nodes of the model now known, and the relations between the strains in the plate and the displacements of the individual nodes being on record, expressions are found for the strains in the plate within the cell outline in terms of the known nodal displacements. In the triangular elements these strains are constant over the whole area of the element, while in the quadrilateral ones they vary linearly as functions of  $x$  and  $y$ . These strains may be converted into stresses by the familiar elastic formulae.

It is convenient to have the stresses determined at the nodes. However, different cells meeting at the same node, would have different stresses there, even if the displacement continuity were preserved along the adjacent cell edges. To reconcile the difference, the nodal stresses of the several cells are averaged up, and this average is taken as representing the stress in the plate prototype.

The validity of the stress values so determined depends on the geometry of the cells and of the whole model. In Fig. 1, four equal rectangular cells meet at the node 1, and the averaging procedure appears logical, and is confirmed

in some actual cases by the exact solutions. On the other hand, in Fig. 2 similar averaging of stresses would not be rational, in view of the difference of the angles in the six cells surrounding the node 1. One feels that the contributions of the wide angle cells  $a$  and  $d$  should be greater than those of the others. The uncertainty could be resolved by assignment of appropriate weights to different cells but the basis for such assignment in general is not clear. If the triangles  $b, c, e$  and  $f$  in Fig. 2 are the isosceles right triangles, it appears reasonable to assign the weight one half to each one of them with the weight unity given the triangles  $a$  and  $d$ . The same difficulty is even more in evidence in models involving irregular cell pattern, as in Fig. 3.

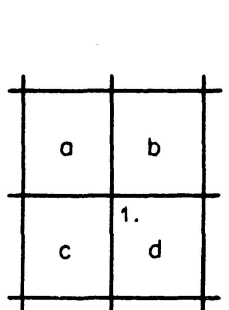


Fig. 1.

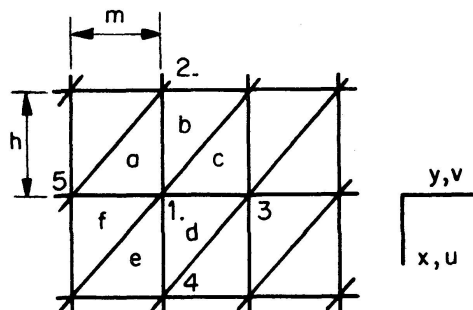


Fig. 2.

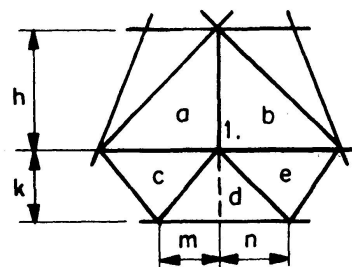


Fig. 3.

Centres of gravity of the cells have also been used as locations for the determined stresses, a procedure requiring no averaging. However, in situations similar to the ones presented in Figs. 2 and 3, the stresses so found are scattered, and an attempt to bring them in line results in approximations and errors. Furthermore, one does not see why these stresses in triangular cells should be referred to the centres of gravity and not to some other locations such as the intersections of bisectors. Difficulty is encountered in application of the method to the boundary nodes, where displacements are available on one side only.

## Method 1b of Nodal Displacements

This is a somewhat crude procedure utilizing in simple form the familiar relations between the strains and displacements. It will be illustrated on the example of the unit strains at the node 1 in Fig. 2. The subscripts in the displacement symbols  $u$  and  $v$  refer to the numbers of the nodes.

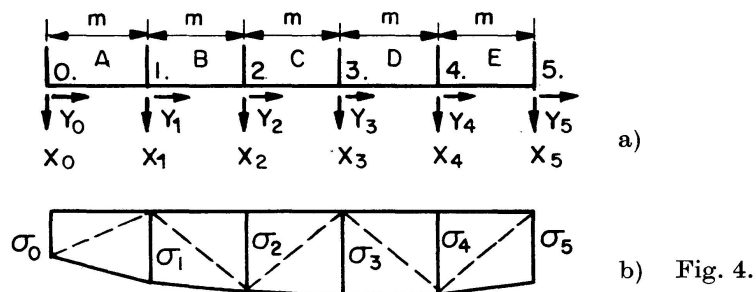
$$\text{Then, } \epsilon_x = \frac{u_4 - u_2}{2h}; \quad \epsilon_y = \frac{v_3 - v_5}{2m}; \quad \gamma_{xy} = \frac{v_4 - v_2}{2h} + \frac{u_3 - u_5}{2m}. \quad (1)$$

The same relations are applicable in Fig. 1, and with some adjustments in Fig. 3. Stresses are found from strains by the familiar elastic formulae. As in Method 1a difficulties are involved at the peripheral nodes.

As to the methods of nodal force concentrations, their direct application is possible only when the edges of the cells form continuous straight lines as in Figs. 1 and 2.

### Method 2a of Nodal Force Concentrations Ref. [3] and [4]

After finding the nodal displacements, the corner forces in all cells are determined by computer as products of the stiffness matrix of the cell and the vector of its nodal displacements. The several cells  $A, B, C, D$  (Fig. 4) are placed in line and the total nodal concentrations  $X$  and  $Y$  are found by adding up the corresponding values in the adjacent cells.



The stress diagram in the plate is assumed to have a polygonal form. Each intermediate nodal concentration, normal or tangential, is converted into a triangular area with the base  $2m$  of the stress diagram directly underneath the node. Thus, with the thickness of the plate  $t$ ,

$$\sigma = \frac{X}{mt} \quad \text{and} \quad \tau = \frac{Y}{mt}. \quad (2)$$

This disposition of the normal concentration  $X$  is in full agreement with statics. Additional justification, equally applicable to the tangential concentrations  $Y$ , is provided by the consideration of proximity, i.e., the plate stresses are placed, quite properly, close to the location of their source. Some modifications of the method outlined here are usually needed at the edges, being demanded by statics.

### Method 2b of Nodal Force Concentrations

This seemingly more rational procedure involves solution of simultaneous equations, and is the reverse of the one used in the assembly of the internodal stresses into the nodal concentrations by the laws of statics.

With a polygonal normal stress diagram (Fig. 4) the following relations hold:

$$\begin{aligned} X_0 &= \frac{1}{6}(2\sigma_0 + \sigma_1)mt, \\ X_1 &= \frac{1}{6}(4\sigma_1 + \sigma_0 + \sigma_2)mt \\ \text{and in general} \quad X_n &= \frac{1}{6}(4\sigma_n + \sigma_{n-1} + \sigma_{n+1})mt. \end{aligned} \quad (3)$$

Here the number of the unknown stress values  $\sigma$  in each row of nodes equals the number of equations, as well as the number of the known concentrations  $X$ .

Similar relations may be written between the tangential concentrations  $Y$  and the shearing stresses  $\tau$ , although in this case, they are based not on statics but on the considerations of proximity.

When the stresses at the edges are zero (as in case of shear stresses), or when the stress diagrams are symmetrical or antisymmetrical, the number of equations exceeds the number of the unknown stresses and then it is necessary to introduce additional parameters, presenting the stress diagram in the shape of the arcs of parabolae instead of straight lines. The details of this procedure will not be described here.

The force concentration methods, especially the latter one, are equal in precision to the nodal displacement methods in conditions described by Fig. 1, and are superior to them in conditions of Fig. 2. The methods are not directly applicable where the cells are unaligned or irregular as in Fig. 3.

### Rectangular Cells of Variable Sizes

In models composed of rectangular cells of different sizes (Fig. 5) determination of stresses by the Methods 1a, and 1b, is imprecise for the reasons explained earlier. Inaccuracy is also inherent in Method 2a, because with the normal stress determined by the formula  $\sigma = \frac{2X}{m+n}$ , the resultant of the two stress triangles immediately under the node does not coincide with it, and for this reason is not statically equivalent to the nodal force. The method 2b is fully applicable, although the Eqs. (3) should be modified for the different sizes of cells. Generally speaking, however, cells of variable size and shape are not recommended, except when they are demanded by some special and irregular shapes of the prototype.

### Identical Cells Differently Oriented

The triangular cells in the model of Fig. 2 have their bases oriented alternately up and down. In Fig. 6 similar triangular cells are arranged with four different orientations. The latter model, unlike the one in Fig. 2 is not directly suitable for stress analysis by the Methods 2a and 2b because its repeating section consists of two cells instead of one, and an adequate method of conversion of two adjacent nodal concentrations into statically equivalent stress diagram in the plate is not apparent. Cell model of Fig. 6 is thus inferior to that of Fig. 2.

### Cell Symmetry

Although the model of Fig. 2 is made of triangular cells, two adjacent cells (Fig. 7) form a rectangle, which may be used as a single equivalent element. The  $8 \times 8$  stiffness matrix of such rectangular cell may be easily formed from the  $6 \times 6$  matrices of the triangular cells composing it. The terms of the stiffness matrix of such "compound" rectangular cell are however, different from those

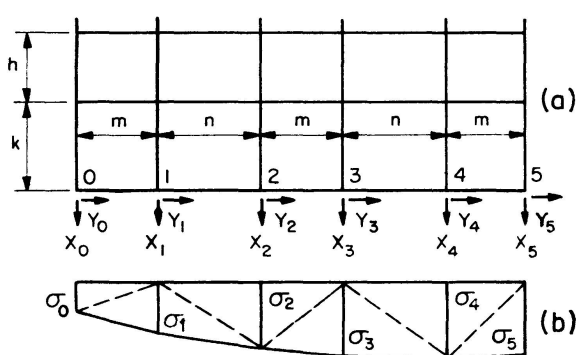


Fig. 5.

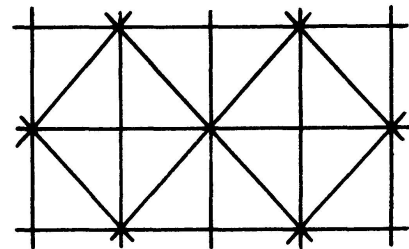


Fig. 6.

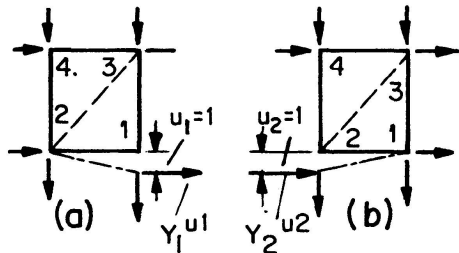


Fig. 7.

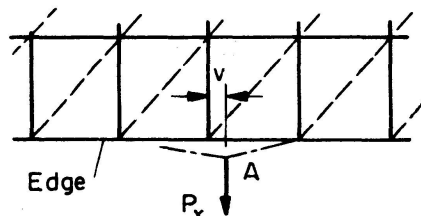


Fig. 8.

of the "straight" rectangular cell. The important feature in this difference is lack of structural symmetry in the compound cell. Thus the corner forces  $Y_1^{u_1}$  and  $Y_2^{u_2}$  in Figs. 7a) and b) are not equal and opposite in sign as they should be and as they are in a "straight" rectangular cell. From this it follows that application of a vertical load at the node  $A$  on a straight boundary of the model (Fig. 8) results in nonvertical displacement of this point. Similarly, a vertical load applied inside a compound cell model, with diagonal intercell boundaries slanting the same way, also produces a non-vertical displacement. On the other hand, with the cell pattern symmetrical about the  $Y$  axis (Fig. 9) the tendency for the sideways movement under a vertical load is cancelled. The error discussed here and associated with the triangular and compound rectangular cells extends also to stresses. The errors, however, diminish and ultimately vanish on reduction of the cell size.

The described intrinsic deficiencies of cells and cell arrangements extend to non-biaxially symmetrical cells in general. This includes the parallelogram

shaped cells such as the ones in the model of Fig. 10, where as in Fig. 8, an action of the load  $P_x$  results in some transverse displacement  $v$ , in contradiction to the actual behaviour of the plate.

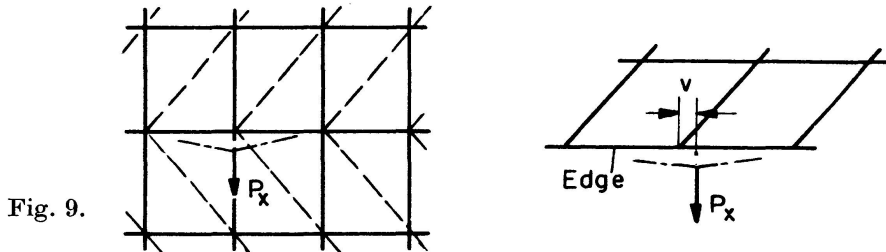


Fig. 9.

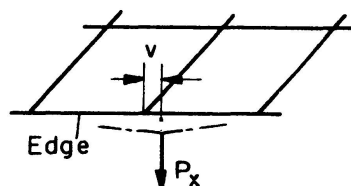


Fig. 10.

### Desirable Shapes of Cells

It may be concluded from what has been said that a model composed primarily of equal rectangular cells is highly desirable. Cells of other shapes, if present, must be confined to the parts of the structure, which cannot be modelled by the principal rectangular cells. Thus model of Fig. 11a for a parallelogram shaped plate is better than that of Fig. 11b composed solely of parallelograms. If the size or shape of the prevailing rectangular cell must be changed in certain areas, the transition region should not be unnecessarily extended.

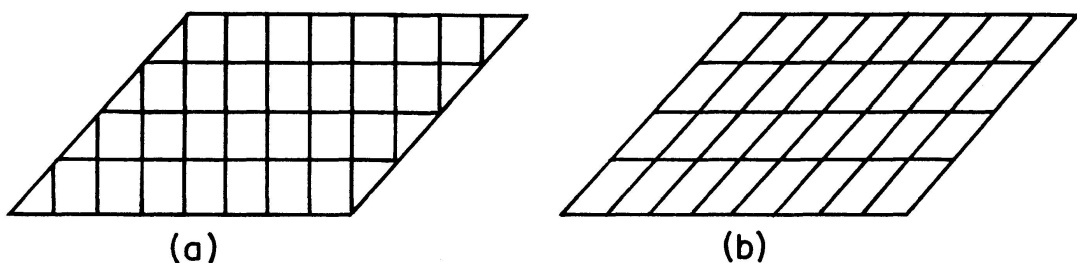


Fig. 11.

One kind of triangles composing the model, the equilateral triangle in view of its triaxial symmetry, would give as good results as the rectangle. The quality of the results with triangles decreases as the angles become unequal. Scattered and irregularly shaped cells lower the precision unless the effect of irregularity is counteracted by the fineness of the mesh size.

The conclusion of an inherent inferiority of non-symmetrical cells must be qualified with reference to the isosceles trapezoids. When such trapezoids are arranged with the bigger bases alternately up and down (Fig. 12) and the model is subjected to a vertical load  $P_x$  at the free edge, the situation is similar to that in Fig. 8 and it is characterized by an erroneous transverse displacement  $v$ . The behaviour of trapezoidal cells is, however, quite different if they are fitted

together with similar orientation of bases in a structure having the form of a complete or partial circular disc (Fig. 13). Here trapezoidal cells represent a rational arrangement, superior in precision to triangles or combinations of triangles and rectangles in spite of possible non-similarity of the cell shapes in different rings. The direction of loads at the nodes makes no difference. Stresses in the plate prototype in the radial and tangential planes may be conveniently calculated by the Method 2a.

Most of the conclusions enunciated here with regard to the effect of the shape of cells are equally applicable to the flexure of plates. Flat trapezoidal cells are quite suitable in stress analysis of shells of revolution both for the membrane and flexure stresses.

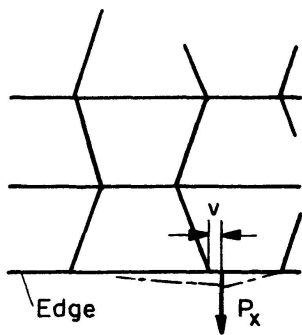


Fig. 12.

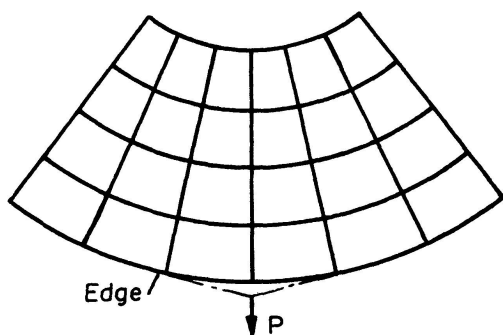


Fig. 13.

### Example

Fig. 14 represents the model of a deep rectangular beam bent in its plane by the uniform load evenly distributed over its top and bottom edges. The beam is supported on the ends by shears distributed parabolically and normal stresses following the law of cubic parabola (Fig. 14 b) whose static effect is

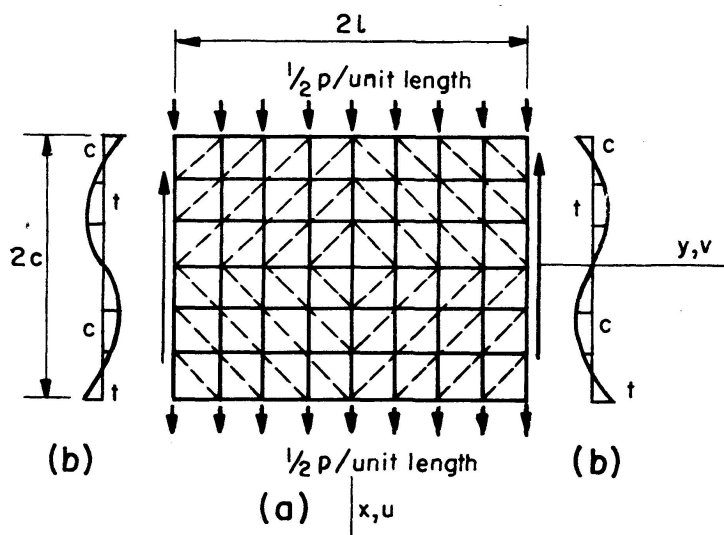


Fig. 14.

zero. This is a slightly simplified version of a problem whose exact solution is known [5]. Models of  $6 \times 8$  and  $12 \times 16$  units with  $\mu = 0.2$  and  $1/3$  were solved using the square cells of TURNER [1] and MELOSH [2] and the compound squares made of triangles, with the hypotenuse oriented the same way in all squares of each quadrant of the model. Three sub-cases of the compound cells were analyzed in which the triangles in the four quadrants were oriented:

- symmetrically in relation to both axes,
- symmetrically with regard to the vertical axis only,
- the same way in all quadrants, i. e., unsymmetrically in relation to both axes.

Two sets of end conditions were used: the known nodal displacements, and the known reactions, assembled into the nodes by the law of the lever. The difference of the two solutions was not substantial, and so only the results of the first one are presented here.

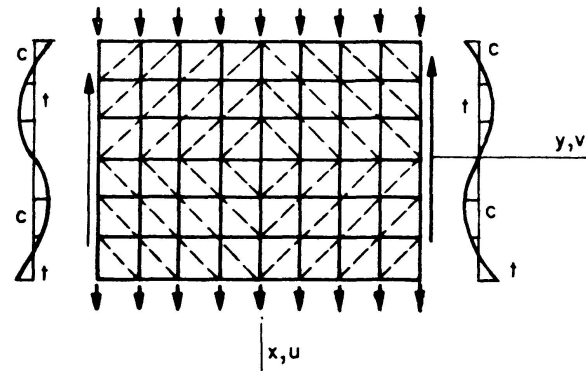
The results are too bulky to be stated in full and so Table 1 presents only

Table 1. % Errors

Symmetrically loaded rectangular beam

$6 \times 8$  Square cells ( $\mu = 0.2$ )

$$\% \text{ Error} = \frac{|\text{True value}| - |\text{Appr. value}|}{|\text{True value}|} \times 100$$



Function	Turner's cell Edges discontinuous		Melosh's cell Edges continuous		Triangular cell Edges continuous	
	Mean	Mean of Max. three	Mean	Mean of Max. three	Mean	Mean of Max. three
Displacement $u$	+0.46	+ 0.80	+0.57	+ 0.87	± 1.13	± 1.87
Displacement $v$	-0.10	- 0.20	±0.23	± 0.46	+ 2.78	+ 5.10
$\sigma_x$	Method 1 a	+7.38	+ 8.43	+7.82	+10.35	± 10.64
	Method 1 b	+9.24	+10.44	+7.82	+10.35	± 15.99
	Method 2 a	±0.31	- 0.71	±0.54	± 0.85	± 13.52
	Method 2 b	±0.42	± 1.01	±0.64	± 1.28	± 19.51
$\sigma_y$	Method 1 a	+4.09	+ 7.35	+5.51	+ 8.28	± 24.02
	Method 1 b	+5.54	+ 8.61	+5.51	+ 8.28	+ 5.87
	Method 2 a	±7.96	-14.37	-5.05	-11.86	- 27.13
	Method 2 b	±4.36	- 7.52	±3.91	- 6.21	+ 29.30
$\tau_{xy}$	Method 1 a	+4.84	+ 6.67	+7.28	+ 9.71	± 5.67
	Method 1 b	+7.28	+10.09	+7.28	+ 9.71	+ 10.89
	Method 2 a	+2.19	+ 3.02	+2.74	+ 3.50	± 5.58
	Method 2 b	±2.73	+ 4.40	±2.80	+ 4.96	+ 8.73

the percentage errors of the displacements and stresses in different solutions. The error is considered positive if the exact value of the function (displacement or stress) is numerically greater than the approximate one. The errors are difficult to generalize because they vary numerically a great deal from node to node, and the exact values, with which they are compared, are themselves widely variable. For this reason two values of the error of each function are stated: the maximum and the mean.

The results are fairly consistent. Here are some observations on the types of cells, methods, and the degrees of inaccuracies of various solutions.

1. The continuity of displacements on the internodal lines is preserved in the Melosh's and the compound cells, but is absent in the Turner's cells.
2. Substantially, the same precision is found with Poisson's ratios 0.2 and 1/3. Theoretically, the value of  $\mu$  in this problem should affect only the displacements and not the stresses. The numerical data presented in the table are based on  $\mu = 0.2$ .
3. The methods of determining stresses from the nodal force concentrations (2a and 2b) prove somewhat better than the ones based on the nodal displacements (1a and 1b), but, unexpectedly, the complicated method 2b shows no advantage over its simple counterpart 2a.
4. Replacement of the  $6 \times 8$  model by the  $12 \times 16$  model, results in reduction of the percentage error approximately four times, i. e., in proportion to the number of cells, when using the Turner's and Melosh's cells, and in a somewhat smaller improvement in the case of compound cells.
5. In nearly all vertical displacements, the error is positive, i. e., the exact values are higher than the calculated ones; in other words, on reduction of the mesh size, the true displacements are approached from below.
6. The quality of the results follows nearly always this order: Turner's, Melosh's and the compound cells, the latter usually lagging behind the first two, – often many times behind.
7. The precision of solutions involving compound cells is not much different on the whole, whether or not the orientation of the triangles in the four quadrants of the model is symmetrical or unsymmetrical about one or both axes. Additional errors, however, are present in unsymmetrical cases on the axes of symmetry of the plate.

### Conclusions

The reasoning presented in this paper justifies the following conclusions, partially confirmed by the results of the example.

1. Proper finite element cells in plane stress must be capable of imitating the deformations of the plate under any uniform stress conditions.

2. The edge continuity of the cells is not an important condition, let alone a necessary condition.
3. On increase without limit of the number of cells, without changing their shape, the displacements in the directions of loads gradually approach the true values from below, irrespective of the presence or absence of continuity on the edges of cells.
4. In the example analyzed, the method of nodal force concentrations proves to be somewhat more precise than the method of nodal displacements.
5. The best precision is obtained with cells of uniform size and particular shapes: rectangles or equilateral triangles, when using rectangular co-ordinates, and isosceles trapezoids in case of polar co-ordinates. Other shapes of cells require finer mesh for an equal precision. Cells of irregular shapes must be restricted to parts of the models (or complete models) which cannot be constructed with the most desirable shapes.

### Notation

$h, k, m, n$	dimensions of cell
$\{K\}$	stiffness matrix of cell
$p$	unit load
$t$	plate thickness
$u, v$	nodal displacements along $x$ and $y$ axes respectively
$x, y$	co-ordinate axes
$P$	nodal force
$X, Y$	components of nodal forces along $x, y$ axes respectively
$\delta$	nodal displacement
$\epsilon$	normal unit strain
$\gamma$	tangential unit strain
$\mu$	Poisson's ratio
$\sigma$	normal unit stress
$\tau$	shearing unit stress

### Acknowledgement

This investigation has been carried out with financial support of the National Research Council of Canada.

### References

1. TURNER, M. J. et al.: Stiffness and Deflection Analysis of Computer Structures. *J. Aeron. Sci.* 23, No. 9, 1956.
2. MELOSH, R. J.: Structural Analysis of Solids. *Proc. Amer. Civ. Eng. ST.* 4, August, 1963.

3. HRENNIKOFF, A.: Solution of Problems of Elasticity by the Framework Method. *J. Appl. Mech.*, A.S.M.E., Dec. 1941.
4. HRENNIKOFF, A.: Framework Method and its Technique for Solving Plane Stress Problems. Publications, International Association for Bridge and Structural Engineering. Vol. 9, 1949.
5. TIMOSHENKO, S.: Theory of Elasticity. McGraw Hill, 1934.

### **Summary**

Various shapes of finite elements used in plane stress analysis are discussed, and the desirability of symmetry is emphasized. Comparison is also made of several methods of determination of stresses. Examples involving different stiffness matrices confirm the enunciated recommendations.

### **Résumé**

Différentes formes d'éléments finis utilisés dans l'analyse du plan des tensions sont discutées et on précise l'avantage de la symétrie. En résumé, on fait donc la comparaison entre plusieurs méthodes de détermination des tensions. Des exemples confirment les déclarations par différentes matrices de déformations.

### **Zusammenfassung**

Verschiedene Formen für endliche Elemente im ebenen Spannungszustand werden erörtert unter Betonung des Wunsches nach Symmetrie. Daneben werden Vergleiche der verschiedenen Verfahren zur Bestimmung der Spannungen gezogen. Beispiele mit verschiedenen Steifigkeitsmatrizen bestärken die ausgesprochenen Empfehlungen.

Leere Seite  
Blank page  
Page vide